Development of Superconducting Electrical Joints for a Superconducting Shim Coil System in the Baryon Antibaryon Symmetry Experiment

Thomas Craig Robert Hepworth

Summer Student Report submitted to the
CERN Summer Student Program

Barbara Maria Latacz
Stefan Ulmer

August 23^{rd}, 2024
CERN, Geneva, Switzerland

Keywords: Superconducting Joints, BASE

Acknowledgements

Having the opportunity to spend this summer as a member of the 2024 CERN Summer Student Program has given me the most awarding personal and professional experience of my entire life. As someone who has never left Canada (other than going to water-parks across the U.S. border) I was able to see new parts of the world and experience many new things while making many close friends.

I would like to thank all of the BASE and BASE-STEP students who I was able to work/spend time with and get to know. Specific thanks go to Tomoka and Julia for welcoming me into our shared office, and to Julia for helping me plan my trip to Heidelberg. Thanks to Matthew for sharing after work beers and sitting in the e-lab and listening to me yell at the cryocooler. Thanks to Bela for the massive help with all areas of this project, offering advice, and joining me in the lab.. Thanks to my supervisor Barbara for trusting me with a very involved project and allowing me to work independently in the 2 month time frame. I really value trust and honesty, and this is something I felt from all of my collaborators and mentors in BASE. I would like to thank the Institute of Particle for sponsoring me to participate in this program. I would also like to thank the Natural Sciences and Engineering Research Council of Canada (NSERC) for awarding me an Undergraduate Student Research Award (USRA) to fund the first half of my summer at TRIUMF, Canada's particle accelerator center, through the University of Winnipeg, and partially fund the second half of my summer at CERN.

Contents

1 Introduction **1**

2 The BASE Experiment **1**
- 2.1 Penning Traps 1
- 2.2 Magnetic Environment of BASE 3

3 Superconducting Shim Coil System **4**
- 3.1 Shimmming and Shielding system 4
- 3.2 Standard Superconducting Joints 5
- 3.3 New Superconducting Joint Concept 6

4 Experimental Setup **8**
- 4.1 BASE Cryocooler 8
  - 4.1.1 Characterization of our Cryocooler 10
- 4.2 Implementation of Cryogenic Hall Probe 12
- 4.3 Test Setup For all Joints 16
  - 4.3.1 Persistent Coil 16
  - 4.3.2 Non Persistent Coil 17
  - 4.3.3 Control Code 18
- 4.4 New Base Joint 19
  - 4.4.1 Acid Treatment 19
  - 4.4.2 Technical Design for Acid Treatment Apparatus 20
- 4.5 New Joint Test 21

5 Next Steps and Summary **22**

List of Figures

1 The motion of a particle in a Penning trap, (black) is the superposition of its three independent eigenmotions: the magnetron motion ν_- (red), the axial motion ν_z (blue) and the modified cyclotron motion ν_+ (green). Figure from [4]. 2

2 Schema of a BASE Penning trap showing the 4 BASE Penning traps. 3

3 Position of the B2 coil (red), B1 coil (green), B0 coil (blue) and the SSC (yellow) on the trap can. Different shades of the same color indicate a reversal of winding direction. The center positions of the Reservoir trap (RT), Precision trap (PT), Analysis trap (AT) and Cooling trap (CT) are indicated. The shimming and shielding system is centered around the Precision trap. Figure taken from [9] 4

4 Cross section through the B2 coil (red), B1 coil (green), B0 coil (blue) and the SSC (yellow). Different shades of the same colour indicate a reversal of winding direction. Figure taken from [9] 5

5 Sketches of oxidation in air of a smooth, single crystal Nb (RRR 30) with many oxide nuclei (a) $\lesssim$ 30 min, (b) $\gtrsim$ 1 week. Details of oxidation processes are discussed in [10]. Figure reproduced from [10]. 7

6 NbTi wire used in [11] when making superconducting joints. 8

7 Joint making process described in [11]. Figure reproduced from [11]. 9

8 Schematic of the cryogenic setup used for the measurements. A two-stage Gifford-McMahon cryocooler is mounted in a vacuum chamber. The test setup (shown in blue) is attached to the second stage of the cryocooler and shielded with a 77K heat shield to reduce radiation impact from the first stage. With this, temperatures around 4K and pressures in the order of 10^{-6} to 10^{-8} mbar can be reached. The interface flanges can be used to connect different devices and to lead out cables for different devices (shown in purple). Figure reproduced from [4]. 10

9 Temperature (K) vs time (hours) during a cooldown with the full test setup mounted to the coldhead. Temperature sensor is mounted to the coldhead as shown in figure 21. Typical operating temperature near 4K is reached in approximately 3 hours. 11

10 Pressure (mbar) vs temperature (K) during a cooldown where the temperature sensor is mounted as shown in figure 21 and the test setup is attached. The minimum point reached on this graph is displayed. 12

11 Temperature (K) vs time (hours) during a cooldown with the full test setup mounted to the coldhead. Temperature sensor is mounted to copper braid. Typical operating temperature near 4K is reached in approximately 3 hours. 13

12 Pressure (mbar) vs temperature (K) during a cooldown where the temperature sensor is mounted to a piece of copper braid and the test setup is attached. The minimum point reached on this graph is displayed. 13

13 Temperature (K) vs time (hours) during a warm-up with the full test setup mounted to the coldhead. Temperature sensor is mounted to the coldhead as shown in figure 21. Room temperature is reached from a starting point near 4K in 24 hours. 14

14 Circuit board (1) designed and described in [12] which controls a Toshiba THS119 Hall probe (2). Picture taken from [12]. 15
15 Hall probe mounted inside of the test setup. 15
16 Circuit of our superconducting persistent coil. Blue lines indicate wires which are superconducting during operation and red wires denote those which are normal conductors. Diagram taken from [4]. 16
17 A loading joint which I made, following the procedure in [9]. The NbTi wire is densely wound around a thicker copper wire, then a thinner copper wire is wound around this to ensure a high contact pressure. This is then soldered to a copper wire, which is the connection to the power supply. 17
18 Pictures of the devices used to test BASE superconducting joints. These devices were on the cryocooler rack as of 23/08/2024. 19
19 A PTFE racket I made for the acid treatment of NbTi wires. **NOTE: Do not use PTFE tape in this setup. It can trap acid and lead to injury. Instead PTFE screws should be used on the bottom.** 20
20 Possible vacuum chamber to store the racket with NbTi wires mounted. This is needed for long term storage of wires if we are not permitted to do our own acid treatments. 21
21 Picture showing the mounting position of a temperature sensor which I would refer to as "mounted on the coldhead". The test setup in not yet attached in this photo. 28

1 Introduction

The standard model of particle physics has been observed to be both incredibly successful and incomplete at the same time. Despite its success, it is unable to correctly predict the observed baryon asymmetry in the universe, known as the baryon asymmetry problem. Modern particle physics experiments investigate physics beyond the standard model by making measurements of fundamental predictions made by the model.

BASE makes world-leading high-precision measurements on protons/anti-protons as a search for CPT symmetry violation. They make these measurements inside of Penning traps. One possibility is to test the CPT invariance theorem, which states that a particle is invariant under combination of charge conjugation (C), parity transformation (P), and time reversal (T). This is true for any local relativistic point-particle field theory, which means that testing CPT invariance tests the most fundamental assumptions of our current understanding of Nature [1]. BASE tests CPT by comparing fundamental properties of particles and anti-particles. BASE measures the anti-proton-to-proton charge to mass ratio [2] and the comparison of the proton and antiproton magnetic moment [3].

BASE compares the charge to mass ratio of protons and antiprotons by testing the equation

$$\frac{q_p}{m_p} = -\frac{q_{\bar{p}}}{m_{\bar{p}}}, \tag{1}$$

where the quantities are measured through the free cyclotron frequency

$$\nu_c = \frac{qB}{2\pi m} \tag{2}$$

for a particle in a Penning trap [2].

The magnetic moment of protons and anti-protons is measured via

$$\frac{g}{2} = \frac{\nu_L}{\nu_c} \tag{3}$$

where ν_L is the Larmor frequency and ν_c is the free cyclotron frequency.

This report discusses work towards the improvements of systematic magnetic field effects which are holding back these two precision measurements.

2 The BASE Experiment

2.1 Penning Traps

Penning traps are limited by any external fluctuations which disturb the fields being set by the traps.

Penning traps use strong magnetic fields combined with a quadrupole electric field to trap particles in three dimensions [2]. There is a magnetic field along the z-axis of the trap which

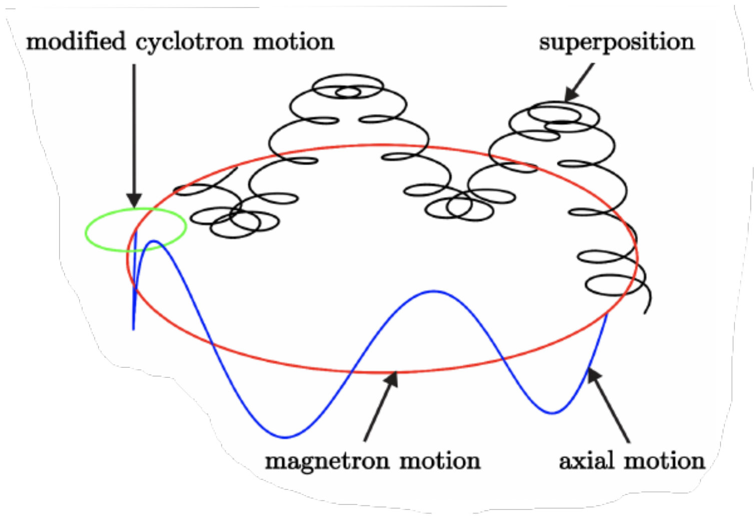

Figure 1: The motion of a particle in a Penning trap, (black) is the superposition of its three independent eigenmotions: the magnetron motion ν_- (red), the axial motion ν_z (blue) and the modified cyclotron motion ν_+ (green). Figure from [4].

radially confines the particle. The motion along the z-axis of the trap itself is restricted by the electric quadrupole potential

$$V(\rho, z) = V_R C_2 (z^2 - \frac{\rho^2}{2}) \tag{4}$$

where z and ρ denote the particles axial and radially position respectively ($\rho^2 = \mathrm{x}^2 + \mathrm{y}^2$), C_2 is a trap specific parameter and V_R is the ring voltage, the difference between the voltage of the ring and end-cap electrodes [5].

These fields create three distinct eigenmotions, shown in figure 1 which completely define the motion of the particle.

These three distinct eigenmotions are:

1. axial motion. This is defined by equation 4 which leads to a harmonic oscillator with frequency:

$$\nu_z = \frac{1}{2\pi}\sqrt{2C_2 V_R \frac{q}{m}}. \tag{5}$$

2. The particle's magnetron mode. This is a result of an $\vec{E}\times\vec{B}$ force (Cite) which has frequency

$$\nu_- = \frac{\nu_c}{2} - \sqrt{\frac{\nu_c^2}{4} - \frac{\nu_z^2}{2}}. \tag{6}$$

3. Lastly modified cyclotron motion. This is a result of the component of the electric field which points radial outwards and affects the free cyclotron motion. The modified cyclotron frequency is

$$\nu_+ = \frac{\nu_c}{2} + \sqrt{\frac{\nu_c^2}{4} - \frac{\nu_z^2}{2}}. \tag{7}$$

These three frequencies completely define the particles motion. The particles cyclotron frequency can then be determined for properly aligned penning traps from the invariance theorem [6]

$$\nu_c^2 = \nu_+^2 + \nu_-^2 + \nu_z^2. \tag{8}$$

In the BASE experiment, the following frequency values are used [2]

$$\nu_- \approx 6.9 \text{ kHz} \ll \nu_z \approx 640 \text{ kHz} \ll \nu_+ \approx 29.6 \text{ MHz} \tag{9}$$

Figure 2 shows the BASE Penning trap stack and the 4 different traps currently used

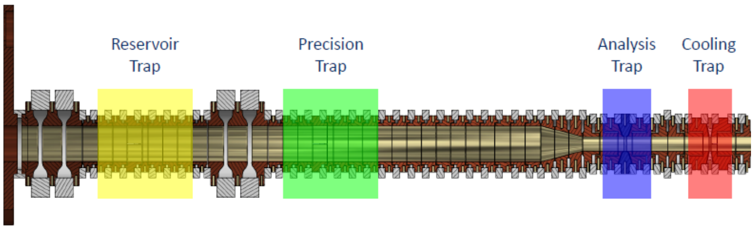

Figure 2: Schema of a BASE Penning trap showing the 4 BASE Penning traps. .

by BASE. The Reservoir Trap is for storing antiprotons, the Precision Trap houses a very homogeneous magnetic field for precision measurements, the Analysis Trap is for spin state identification using the continuous Stern-Gerlach effect, and the Cooling Trap is for making very low energy protons and antiprotons. More details can be found in [7, 8].

2.2 Magnetic Environment of BASE

The magnetic inhomogeneity around the center of the BASE Precision Trap used to measure the cyclotron frequency is approximated as

$$B_z(z) = B_0 + B_1 \cdot z + B_2 \cdot z^2 \tag{10}$$

in the axial direction. B_0 is the static magnetic field, B_1 denotes the magnetic field gradient and B_2 is the quadratic magnetic field inhomogeneity [9]. The main systematic trap-related frequency comes from the cyclotron frequency shifts induced by the B_2 value. B_1 is also contributes to smaller frequency shifts. This was the dominant systematic effect in the 16 ppt charge to mass ratio made by BASE in [2]. Thus being able to impose a value of $B_1 = 0$ and $B_2 = 0$ in the trap would greatly improve the measurement precision for both charge-to-mass and g-factor measurements. To do this BASE has implemented a superconducting shim coil system to allow the tuning of the axial magnetic field [9, 5]. The remainder of this report discusses this system, and the development of improved superconducting joints required to tune the B_1 and B_2 coefficients to 0. Section 3 discusses why these improvements are necessary.

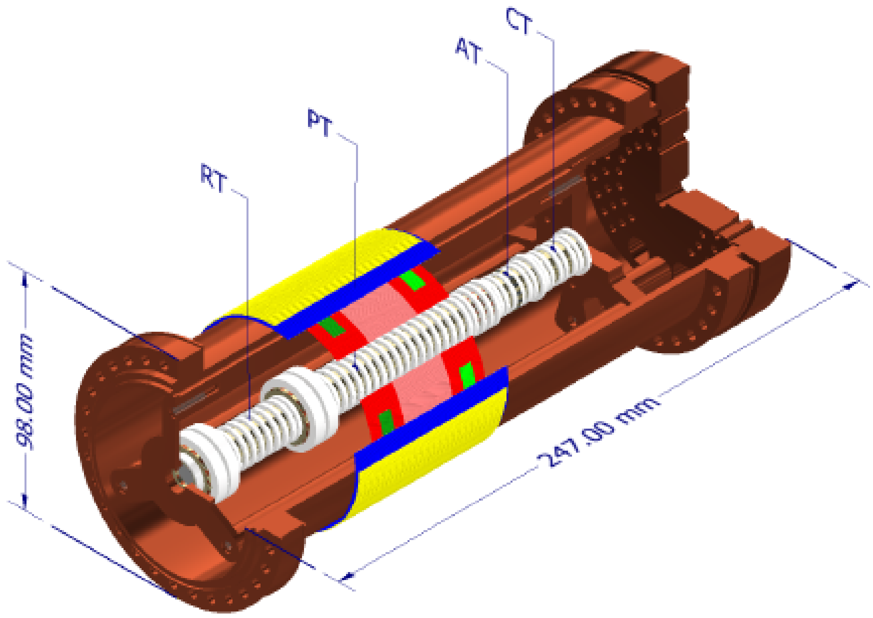

Figure 3: Position of the B2 coil (red), B1 coil (green), B0 coil (blue) and the SSC (yellow) on the trap can. Different shades of the same color indicate a reversal of winding direction. The center positions of the Reservoir trap (RT), Precision trap (PT), Analysis trap (AT) and Cooling trap (CT) are indicated. The shimming and shielding system is centered around the Precision trap. Figure taken from [9]

3 Superconducting Shim Coil System

3.1 Shimmming and Shielding system

The BASE shimming coils are used to control the main systematic of the frequency measurements made in Penning traps. There are three coils which provide the ability to tune B_0, B_1, and B_2 in the expansion shown in equation 10. These coils are to each be responsible for one coefficient, and only make minor contributions to the different order coefficients [9]. A picture of the shimming coil and self-shielding coil (SSC) system is shown in figure 4. Each of the three shim coils are made with the same fundamental design. This is further described in section 4.3.1. The specific design dimensions of each coil are fully described in [9].

It was found that the superconducting persistent joints in this system can operate with loading current of up to 250 mA before they fail to operate persistently [9]. For B_2, this is not a problem as around 67 mA of current must be loaded into the system. This is not the case for B_1 which needs over 1 A of current to tune the value to zero [9]. This does not limit a g-factor measurement to the 100 p.p.t level, but it will limit even more precise future measurements. Thus, the motivation for this project is straightforward: improve the BASE superconducting joints such that they can handle the loading current required to tune B_1 to zero along with the already zero B_2. A joint that can handle much more current along with a several Tesla magnetic field while demonstrating stable persistent operation must be developed to take a further step towards g-factor measurements of protons and anti-protons.

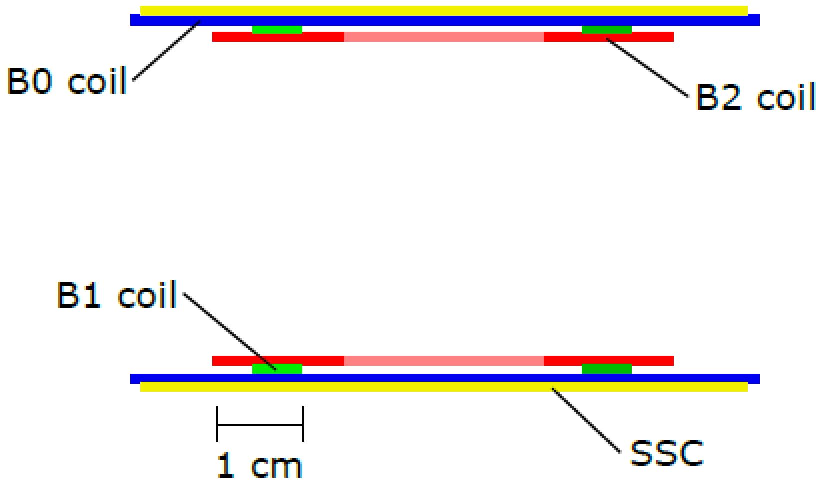

Figure 4: Cross section through the B2 coil (red), B1 coil (green), B0 coil (blue) and the SSC (yellow). Different shades of the same colour indicate a reversal of winding direction. Figure taken from [9]

3.2 Standard Superconducting Joints

To make the superconducting joints currently implemented in the BASE experiment, the following process developed by Jannek Hansen is followed:

1. hold NbTi wire in clamp (use tape to prevent metal on metal contact)
2. sand ends to remove all insulation from a few cm of wire.
3. solder the ferrule
   (a) use a small inner diameter ferrule
   (b) insert both ends of NbTi wire and pull a few cm through all the way
   (c) solder
4. clean ends of wire with acetone
5. clean spot welding needle and check it is flat under microscope
6. clean spot welder with acetone
7. twist ends of wire together
8. clean with acetone
9. check under microscope
10. cut off most of twisted wire, leaving only a few mm
11. spot weld for 2 ms using 1% power

12. if the joint is dark then it is not good. It should be a shiny small bulb.

I made some of these joints to familiarize myself with the process. Unfortunately, we ran out of Argon gas for the spot welder so I was not able to produce a joint which was proficient enough upon inspection to test inside of the cryocooler given the limited time frame I was working under. Pictures and further details of such joints can be found in [9, 4, 5].

3.3 New Superconducting Joint Concept

In comparison to superconducting magnets, superconducting joints have not yet reached such a high technological importance [10]. These joints must maintain operational in very high vacuum while sustaining several thermal cycles between room temperature and cryogenic temperatures [10]. Halbritter lists the following properties as crucial properties of materials used in superconducting devices that are exposed to locally high current densities (such as joints or rf cavities) [10].

1. stable, dielectric oxides which protectively coat the superconductor
2. mechanical ruggedness to support the metal-oxide system
3. long-time stability throughout repeated thermal cycling
4. homogeneity of the superconductor and the dielectric coating with a sharp transition between them.

These are among some of the reasons that Nb-alloy superconductors are among the most widely used for the previously discussed specific applications for superconductors. In addition to this Nb is attractive since it has a high critical temperature for a cryogenic superconductor of $T_c \approx 9.3$ K.

It has been observed that NbTi oxidizes, and a variety of Niobium-Oxides can form leading to loses in superconductivity [10]. Figure 5 shows a sketch of the proposed oxidization process of Nb, where a formation of an NbO layer between the Nb and Nb2O5 layers is meant to account for the loses in superconductivity [10].

From our perspective, we are most interested in removing these oxide layers which form through oxidation in air at room temperature. Halbritter reports that when measuring strain-free Niobium films with an Residual Restivity Ratio (RRR) greater than 100, you will not see any loses in T_c if your Nb_20_5 layer does not exceed 2 nm [10]. It is then obvious that if we want to maintain optimal superconducting properties in our superconducting joints, efforts to remove Niobium-Oxide layers are worth investigating to allow for a purely Nb superconductor which has optimal superconducting properties.

We plan to remove these Nb-Oxide layers via acid treatment of our NbTi wire. This will be done in the CERN acid lab, where they also treat CERN's superconducting rf cavities with the same process (cite something). This process uses a mixture of H_3PO_4 50% v/v, HNO_3 25% v/v and HF 25% v/v. We plan to combine the treatment of our NbTi wire

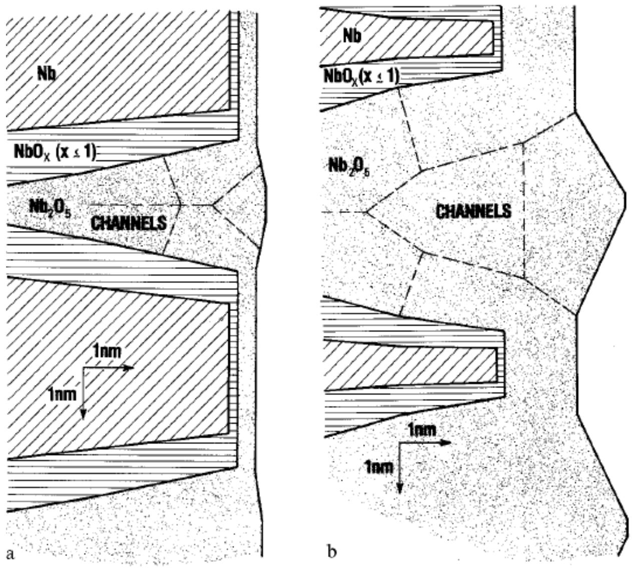

Figure 5: Sketches of oxidation in air of a smooth, single crystal Nb (RRR 30) with many oxide nuclei (a) $\lesssim$ 30 min, (b) $\gtrsim$ 1 week. Details of oxidation processes are discussed in [10]. Figure reproduced from [10].

with a superconducting joint fabrication method which is new to BASE and described in [11]. They outline a method in which two different superconducting Pb-Bi solders were used in the development of superconducting joints designed for persistent mode operation. Note that while they created their joints in an inert environment to avoid oxidation, we took the approach of acid treatment to remove oxidization simply due to the facilities available to us at CERN and our ability to store wires and joints under vacuum afterwards to prevent oxidization while test joints are developed and pending installation in the BASE experiment. As discussed in [10], oxide layers are forming withing 30 minutes, so it is critical for us to store the wires in vacuum within this time frame. Patel et. al use a multi-filament NbTi wire supplied by Luvata, which is shown in figure 6.

This is in contrast to our proposed superconducting joints where we use single strand NbTi wire where no Cu matrix is present (confirm with Bela). Two solders, $Pb_{44.5}Bi_{55.5}$ and $Pb_{42}Bi_{58}$ were tested and were estimated to both have critical temperatures near T_c = 8.5 K [11]. Since NbTi has a T_c = 9.3 K the slightly lower critical temperature of the PbBi solder is not a concern regarding how it may affect the operating temperature of our superconducting joints.

Figure 7 outlines the joint fabrication process followed for the multi-filament Cu matrix NbTi conductors. They first begin by removing the layer of wire insulation using abrasive paper. In contrast, we will have removed this layer before our aforementioned acid treatment of our single-strand NbTi wire. Then the wire must be cleaned using acetone before being immersed in an Sn bath at 350° C for 80 minutes. The now Sn coated NbTi wires are then placed in a molten $Pb_{44.5}Bi_{55.5}$ or $Pb_{42}Bi_{58}$ bath at 350° C for 80 minutes. These wires are then removed from the bath and allowed to naturally cool in air. The wires were then placed

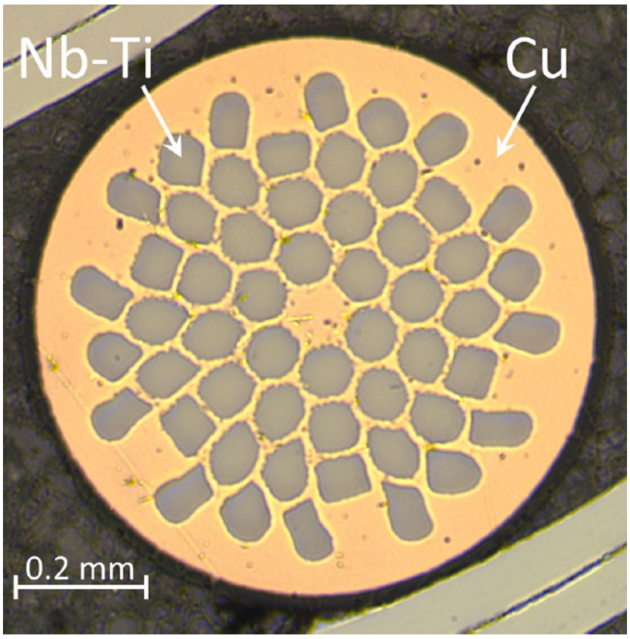

Figure 6: NbTi wire used in [11] when making superconducting joints.

in a copper tube and immersed in a second Pb-Bi bath at 200° C for 10 minutes. This was done for a Cu tube with dimensions of 5.7 mm, 8 mm and 53 mm (I.D., O.D, and height) [11]. The joint is again allowed to cool to room temperature, where upon cooling you have created a superconducting joint. Note that during this study argon was continuously flowed over the joint during heating and cooling processes [11].

It was found that joints made using these methods had $I_c > 200$ A in a field < 1.43 T at 4.2 K for a joint made using $Pb_{42}Bi_{58}$ solder and $I_c > 200$ A in a field < 1.58 T at 4.2 K using $Pb_{44.5}Bi_{55.5}$ [11]. The best of the 5 joints made (this one with $Pb_{44.5}Bi_{55.5}$ solder) showed an $I_c = 136$ A in 1.65 T at 4.2 K [11]. Persistent mode operation of a solenoid coil was successfully demonstrated using these persistent joints [11]. Currently implemented BASE persistent joints can operate persistently up until $I_c = 300$ mT. If implementing this joint fabrication method gave us only some% of the described critical current, we would be able to successfully tune our B_1 parameter to 0 as described in section blah. This study is also of interest as such a method using single strand NbTi wire which we will use when creating joints with this fabrication method have not been studied.

4 Experimental Setup

4.1 BASE Cryocooler

In the BASE electronics lab two ultra high vacuum cryogenic setups are available as shown in figure 8 for the testing of superconducting joints, or more generally any other setup which requires testing under vacuum/cryogenic temperatures.

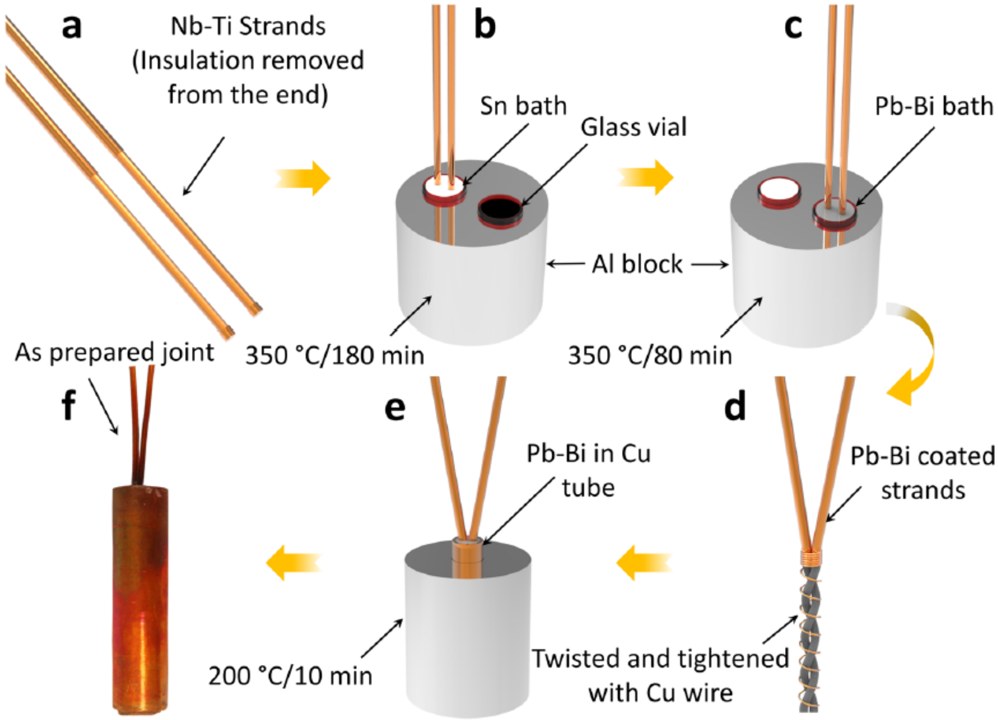

Figure 7: Joint making process described in [11]. Figure reproduced from [11].

The test stand which I used was made up of a two-stage Gifford-McManhon cryocooler stored inside of a vacuum chamber. This chamber has several interface flanges used as cable feed through and connection interfaces for devices such as temperature sensors, pressure gauges, and Hall probes. We pump on the vacuum chamber using a Agilent TPS compact vacuum pumping station, and a Sumimoto RDK408D2 cryocooler is connected to the top of the chamber. Pressures of 10^{-6} mbar and temperatures of around 4K were achieved with this setup in [4]. Using this setup I was able to improve upon these values to lower pressures and temperatures which is further discussed in section 4.1.1.

The first stage of the cryocooler mediates between room temperature and an intermediate cold stage, typically being held between 77-100 K. Without this stage it would be very challenging to cool from room temperature directly to 4 K. This stage has a shield wrapped in foil mounted to it which acts to reduce heat transferred to the second 4 K stage via radiation. Super-insulating foil is typically wrapped around the 4K stage and test setup to further shield from radiation. Temperature measurements should be consistently made during all operating time of the cryocooler. This is done using two Keithley 2000 digital multi-meters (DMM). Temperature sensors are typically placed on the bottom of the shield, and on the 4 K interface, but they can be placed anywhere inside of the vacuum in principle. Pressure is measured using a Pfeiffer compact full-range gauge, which is read out by a Pfeiffer TPG 262 single gauge controller.

The environment provided by this cryocooler is similar to that of the BASE experiment

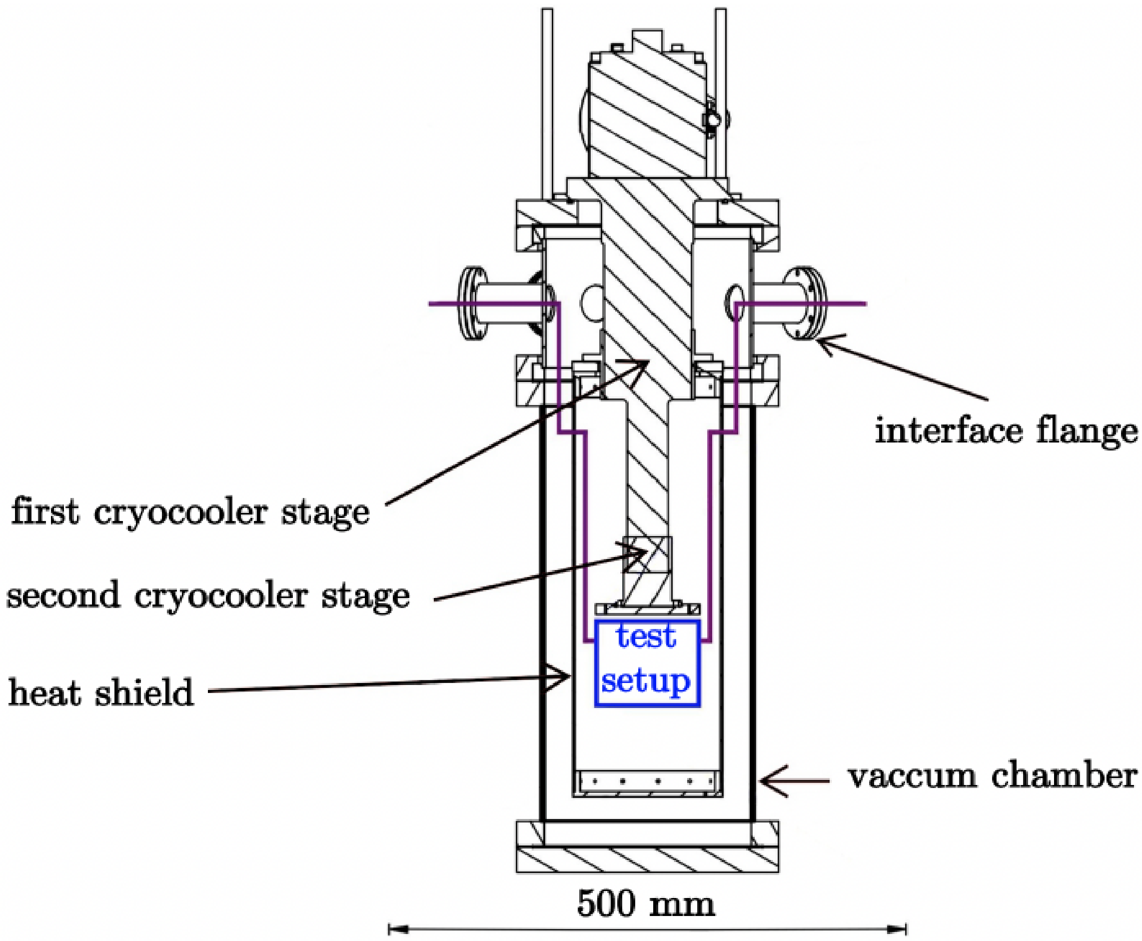

Figure 8: Schematic of the cryogenic setup used for the measurements. A two-stage Gifford-McMahon cryocooler is mounted in a vacuum chamber. The test setup (shown in blue) is attached to the second stage of the cryocooler and shielded with a 77K heat shield to reduce radiation impact from the first stage. With this, temperatures around 4K and pressures in the order of 10^{-6} to 10^{-8} mbar can be reached. The interface flanges can be used to connect different devices and to lead out cables for different devices (shown in purple). Figure reproduced from [4].

and can be used to make comparative measurements for equipment being developed in this report.

4.1.1 Characterization of our Cryocooler

Something relevant to all researchers who may work in the BASE electronics lab is the performance of the cryocoolers which are available. I completed my work using the “old” cryocooler. The most recent operational data posted in the electronics lab for BASE members dates back to 2013. Because of this, I studied the pressure which can be achieved as well as the cooldown and warm-up times of the cryocooler when the test setup is attached. The test setup is a good general representation of the maximal heat load which could exist on the cryocooler for any BASE experiments. In addition, a study of the cooldown time of our test setup itself was made to show the time difference between cooling the coldhead and the test setup.

Figure 9 shows temperature over time of the coldhead with the test setup attached. It is seen that a cooldown of the coldhead to approximately 4 K takes 3 hours and the shield is at 220 K at this time. Note that the shield is ideally as cold as possible during operation, but the temperature of the coldhead dominates above all else so it is used as the metric for cooldown time. Additionally, because the shield is rather deformed it is not uncommon to see a noticeable difference in shield cooldown time between runs as it is hard to achieve the same thermal contact in a repeatable fashion.

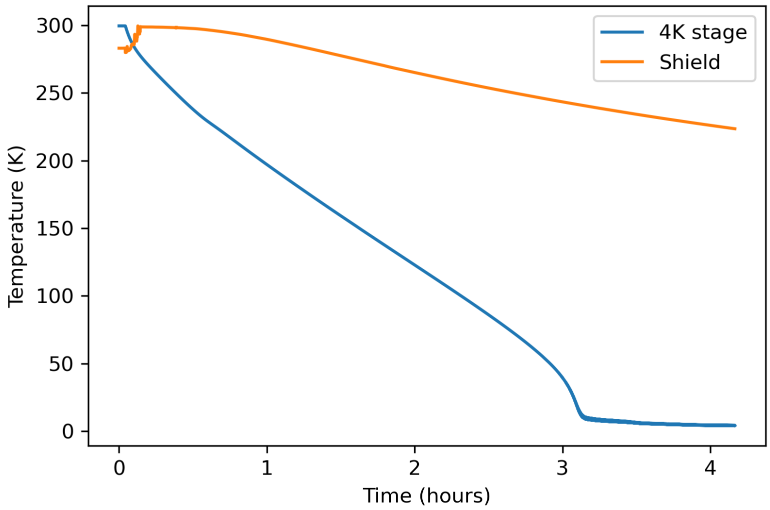

Figure 9: Temperature (K) vs time (hours) during a cooldown with the full test setup mounted to the coldhead. Temperature sensor is mounted to the coldhead as shown in figure 21. Typical operating temperature near 4K is reached in approximately 3 hours.

Figure 10 shows pressure vs temperature during this same cooldown. This demonstrates that pressures on the order of 10^{-7} mbar should be easily achieved, and if the cryocooler operates long enough pressures on the order of 10^{-8} mbar will be reached via cryo-pumping. A temperature of 3.9 K and pressure of 5.89 x 10^{-7} mbar were reached. During a cooldown, it should typically take 1.5 – 2 hours to reach pressures of high 10^{-4} mbar, the pressure at which you should begin your cooldown. If this is not what you observe, then you should be expecting to find a leak somewhere in the vacuum system. After this, you can expect the cryocooler to lower the pressure by 2 orders of magnitude rather quickly, 3 orders of magnitude within a few hours, and 4 hours of magnitude within 12 – 24 hours. If this is the case, then you are successfully operating the "old" BASE cryocooler.

The same plots are now shown with the temperature sensor mounted on a piece of Cu braid near the bottom of the test setup. It is seen that a cooldown of the test setup to

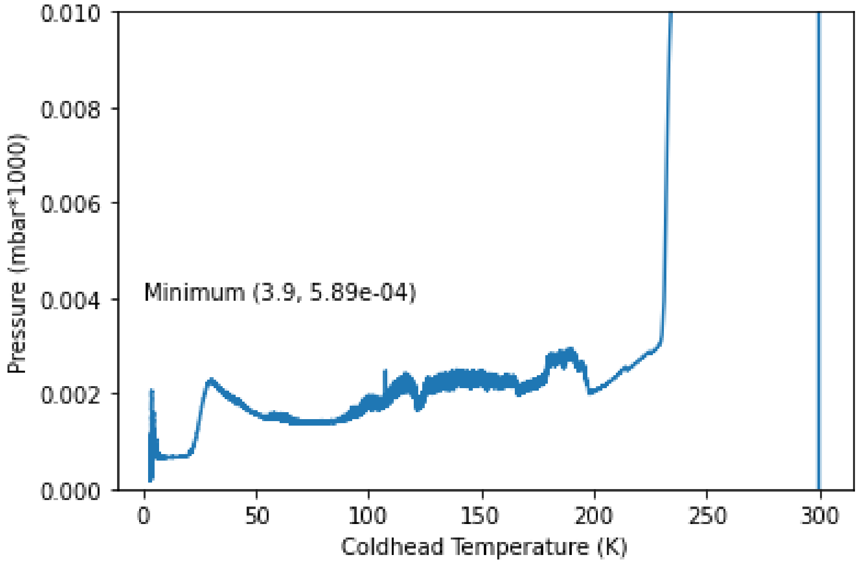

Figure 10: Pressure (mbar) vs temperature (K) during a cooldown where the temperature sensor is mounted as shown in figure 21 and the test setup is attached. The minimum point reached on this graph is displayed.

approximately 4 K takes 3 hours and the shield is at 230 K at this time. The difference between cooldown time between the test setup and the coldhead is negligible. The purpose of this study was to determine if it will take us much longer to cool the test setup, allowing us to test our joints in comparison to the time it takes to cool the coldhead itself. It was confirmed that the temperature sensor being on the copper braid was a good enough representation of the temperature of all parts of the test setup since the loading and persistent joints were measured with a multi meter to have zero resistance. This demonstrates that they were superconducting, and at least below the critical temperature $T_c = 9.3$ K for NbTi.

It is also important to know how long it takes the coldhead to warm-up to room temperature. This time dictates the schedule for which you may have to plan a warm up, if there is specific maintenance you need to complete on a certain date. Figure 13 shows that it takes around one day for the cryocooler to warm up to room temperature. Warm-up time for the test setup is not shown separately, as it would cool in the same time or less in comparison to the coldhead since it is cooled through the coldhead itself.

4.2 Implementation of Cryogenic Hall Probe

As discussed in section 4.3.3, a Hall probe is used to infer the critical current that is in the persistent coil. Previously, a Honeywell SS496A1 hall probe was used to measure the critical current [4]. This hall probe required heating to temperatures of 45 K for it to operate [4]. This introduces an additional challenge in keeping the coil at cryogenic temperatures and introduces temperature dependent errors during measurement sequences. I am implementing a Toshiba THS119 hall sensor which can operate at cryogenic temperatures. This hall

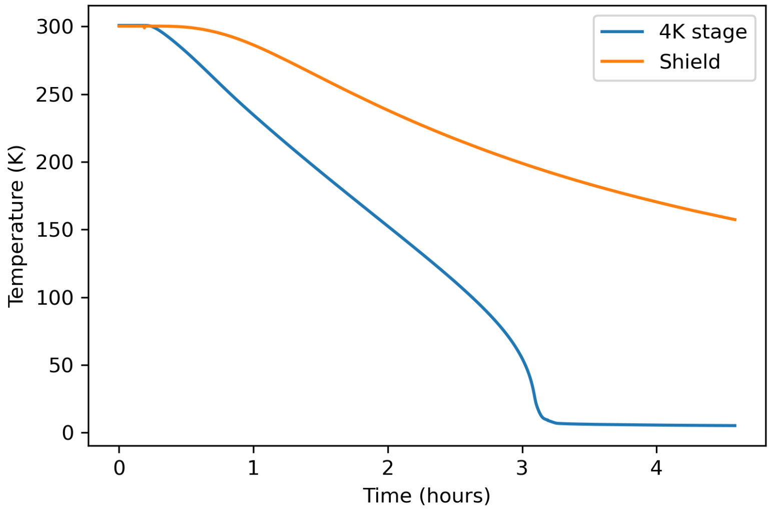

Figure 11: Temperature (K) vs time (hours) during a cooldown with the full test setup mounted to the coldhead. Temperature sensor is mounted to copper braid. Typical operating temperature near 4K is reached in approximately 3 hours.

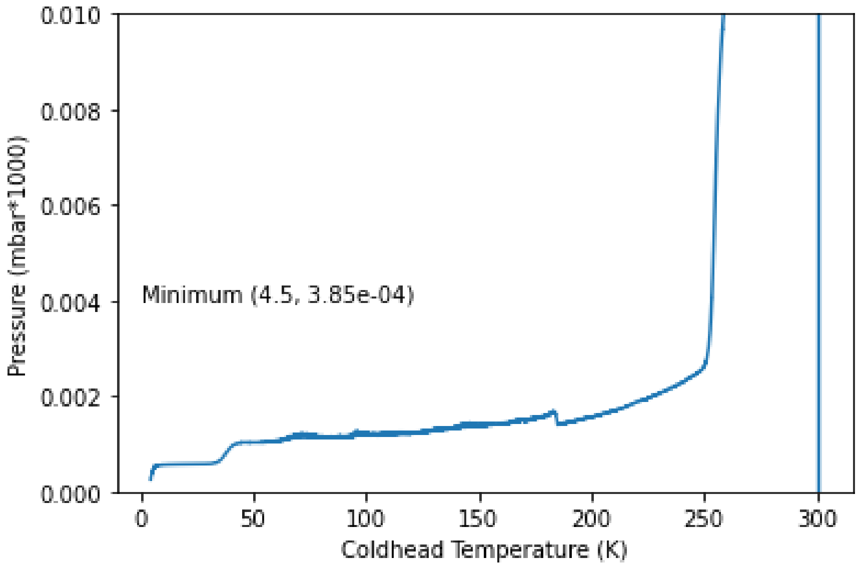

Figure 12: Pressure (mbar) vs temperature (K) during a cooldown where the temperature sensor is mounted to a piece of copper braid and the test setup is attached. The minimum point reached on this graph is displayed.

probe was studied to be suitable for applications in BASE in [12].

Figure 14 shows pictures of the Hall probe and associated circuit board, and the mechanism used to mount it inside of the persistent coil. Figure 15 shows how the Hall probe is mounted inside of the persistent coil. The Toshiba Hall probe is able to make measurements to the precision required for us when testing the persistent joint. It was found to have suf-

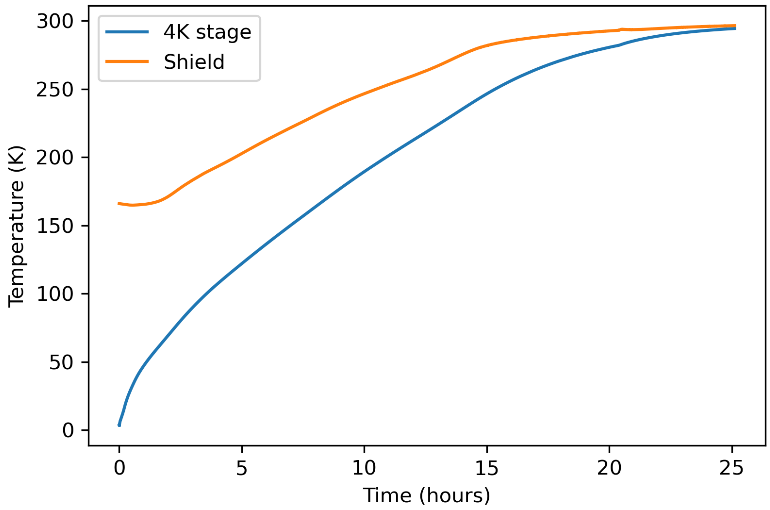

Figure 13: Temperature (K) vs time (hours) during a warm-up with the full test setup mounted to the coldhead. Temperature sensor is mounted to the coldhead as shown in figure 21. Room temperature is reached from a starting point near 4K in 24 hours.

ficiently low noise when measuring magnetic fields below 30 μT while having measurement drifts less than 0.1% over time [12]. It was also found to be very rugged, having no measured performance difference after 30 repeated thermal cycles between cryogenic and room temperatures [12].

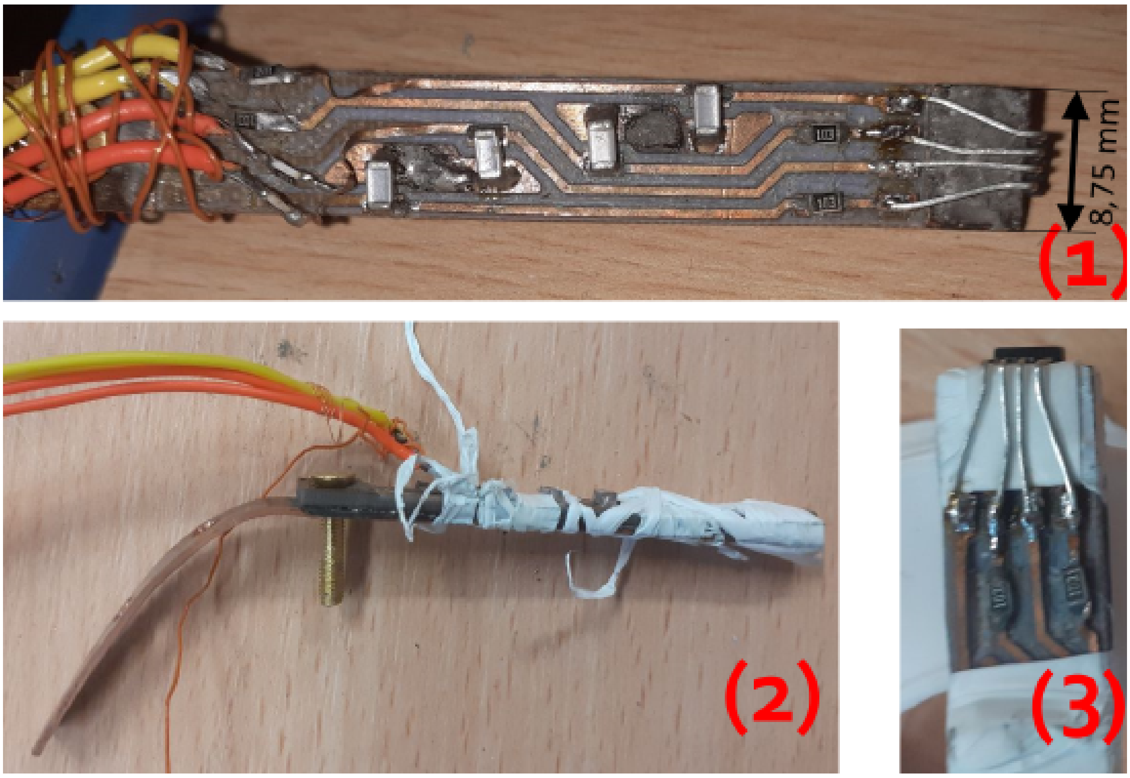

Figure 14: Circuit board (1) designed and described in [12] which controls a Toshiba THS119 Hall probe (2). Picture taken from [12].

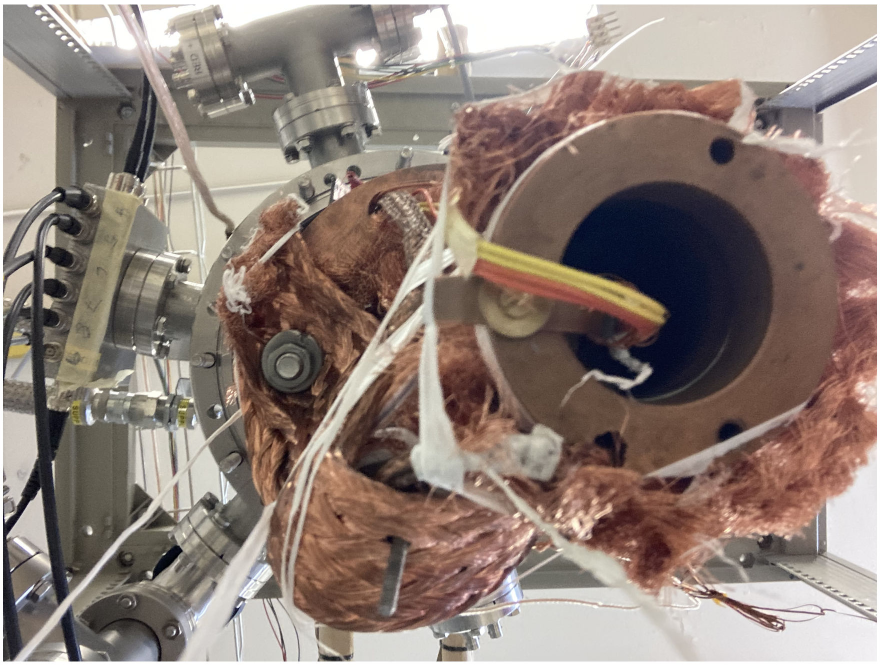

Figure 15: Hall probe mounted inside of the test setup.

4.3 Test Setup For all Joints

4.3.1 Persistent Coil

The Persistent Coil is a superconducting solenoid, designed to operate in persistent mode after being loaded with current. Being able to operate without constant current loading allows for a stable magnetic field, over long time periods. It is made using NbTi wire, which is used in current BASE systems.

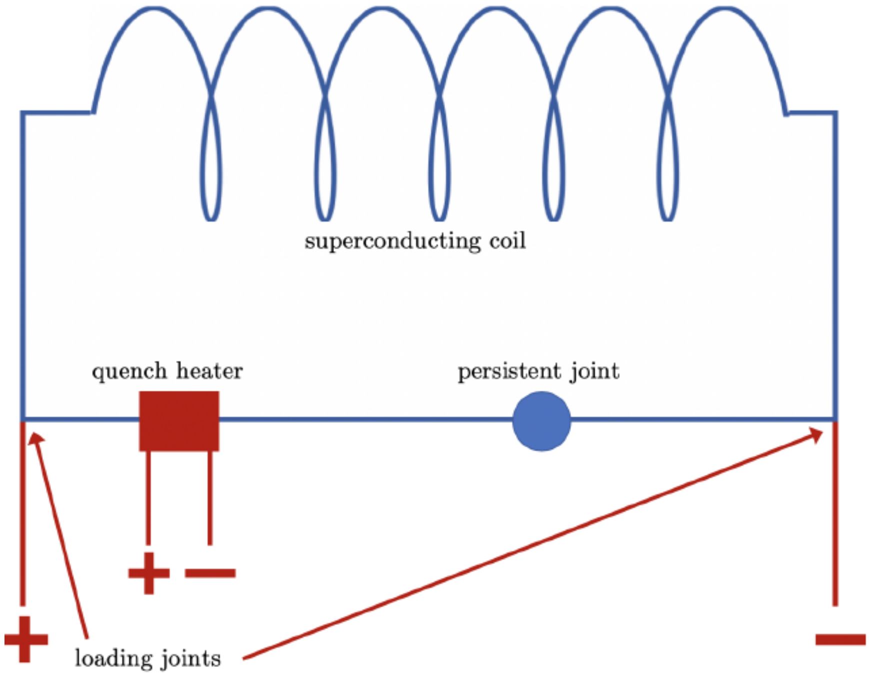

Figure 16: Circuit of our superconducting persistent coil. Blue lines indicate wires which are superconducting during operation and red wires denote those which are normal conductors. Diagram taken from [4].

Figure 16 shows the persistent coil circuit. It is made using:

- a superconducting coil made out of $\phi = 125\mu m$ NbTi single strand wire. This is wound around a copper tube which can mount to the coldhead on the cyrocooler.
- A persistent joint which you plan to test. This of course will vary.
- Two loading joints which connect copper wire to the superconducting NbTi wire.
- A quench heater to locally heat the NbTi wire. I used an 83 Ω resistor. It is important to insulate this with Kapton and PTFE tape so it does not heat other parts of the superconducting coil, causing a quench.

With this test setup any persistent joint can be swapped in for testing. The making of a standard spot welded joint is described in [4]. Since we are trying to improve the persistent joint, it is important to make the loading joints the same each time. The making of a BASE loading joint is described in [9]. A practice loading joint which I made is shown in figure 17. More pictures of loading joints are found in [4].

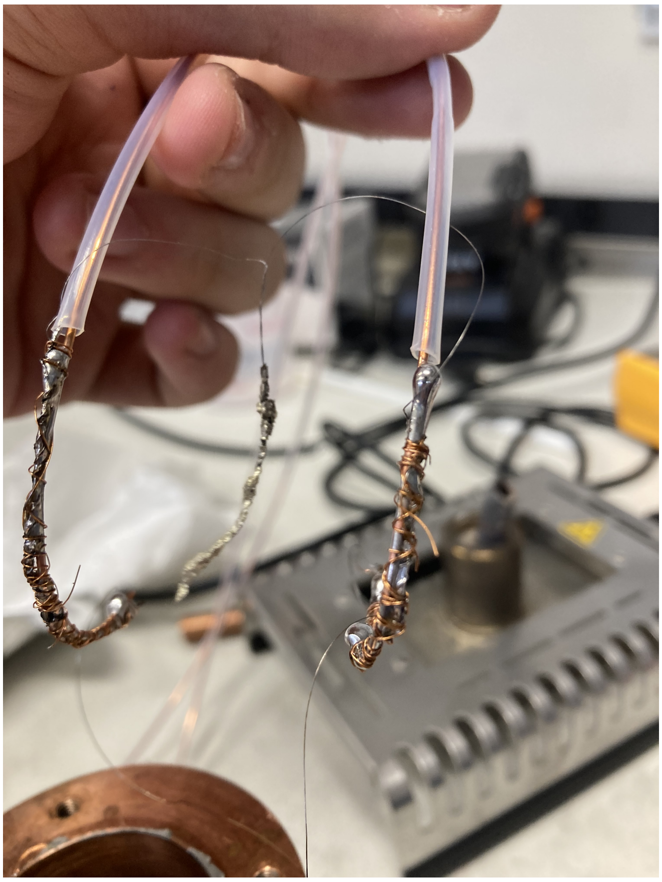

Figure 17: A loading joint which I made, following the procedure in [9]. The NbTi wire is densely wound around a thicker copper wire, then a thinner copper wire is wound around this to ensure a high contact pressure. This is then soldered to a copper wire, which is the connection to the power supply.

It is very important to make sure this setup is properly thermalized. This is done using copper braid and PTFE tape. More details are discussed in [4] and figure 14 shows what a prepared test setup looks like.

4.3.2 Non Persistent Coil

In order to test how a superconducting joint behaves in different external magnetic fields, another coil is required for control over the experiment. This coil is also superconducting, and named the "non-persistent coil" as it is constantly powered during operation. I had to fix the connections for the non-persistent coil as it had many instances of shorting to the copper base. This is something to look out for when preparing a test setup. Proper operation can be checked by measuring the resistance. It should be around 12.85 kΩ. Details of the coil design are found in [4].

4.3.3 Control Code

For the testing of superconducting joints, a labview code needed to be developed. Learning how to program in Labview was an important part of my summer internship. The required code needs the following core functions:

1. Read out two temperature sensors from two Kiethley 2000 digital multimeters via 4 wire resistance measurements.

2. Read out a pressure sensor from a Pfeiffer TPG262 controller.

3. Read out of a Hall-probe output voltage with a Keithley 2110 5.5 digit digital multimeter.

4. Control of the 3 channels on a Keithley 2230G DC power supply.

With these core functions, different measurement protocols can be developed for the testing of any BASE superconducting joint. These devices are on the rack besides the cryocooler and shown in figure 18. These should not be moved that way the incoming BASE student can immediately pickup this code and start working on joint development.

The test procedure used for joints in the current code works in the following way:

1. Apply a current to the quench heater to locally heat the wire above the critical temperature. This causes a loss in superconductivity in this section of the wire. A few mA should usually be sufficient to heat the wire. Depending on the given test joint, this can vary due to the fact that you must not heat other parts of the coil too much.

2. The current then flows through the loading joint and into the coil, which should still be superconducting.

3. The quench heater is deactivated, making the wire superconducting again. This confines the current inside a closed loop.

4. The loading current is disabled and the coil should be producing a stable magnetic field

5. The magnetic field is measured using the Hall probe over varying time scales. An average of many values is taken to account for the noise present in the hall probe.

This procedure follows that outlined in [4], but is described here in more detail in the context of how the code is written. Each of the mentioned steps have different wait times that can be set between them. This is important to consider for the quench heater, as we must be sure that the persistent joint has enough time to become superconducting before the loading current is turned off. The front panel of the code is shown in the appendix.

Figure 18: Pictures of the devices used to test BASE superconducting joints. These devices were on the cryocooler rack as of 23/08/2024.

4.4 New Base Joint

4.4.1 Acid Treatment

The acid treatment used by the CERN acid lab to remove oxide layers from NbTi uses a mixture of H_3PO_4 50% v/v, HNO_3 25% v/v and HF 25% v/v. See the appendix for the acid labs documentation. Based on the specification of removing $1\mu m$/minute from the diameter of the wire under acid treatment, we can develop a systematic study of how much oxide we can remove from the wire and how it affects superconductivity. For the one test joint I made, I do not know how long the wire was treated (not privy do this information). Due to a misunderstanding, we believe the treated wire was left out in air for more than 30 minutes before we picked it up and made it into a joint. We were also made aware that only one end of the wire was treated with acid. We were only able to get one sample treatment of a wire, so these circumstances were the limiting reagent for our ability to produce several joints using the new method of interest.

In order to better control the acid treatments we use, the acid treatments should be done by BASE themselves. This also allows for systematic study of acid treatment which could be used for a technical paper about new BASE superconducting joints in the future. In order to do this, the proper training from CERN must be completed in order for BASE to have permission to use these acids. This should be further investigated for the future of this project as a possible bachelor's thesis.

4.4.2 Technical Design for Acid Treatment Apparatus

If BASE is not permitted to do these acid treatments themselves at CERN, an apparatus is required for the systematic treatment of many NbTi wires. These can then be stored under vacuum and quickly taken it out when a new joint is ready to be made. If BASE were to store 20 of these wires, you could imagine that they would have oxygen exposure after repeated opening and closing of the storage chamber. It is possible that a small layer of oxide could be removed by some other acid such as HNO_3 immediately before the making of a new joint. Removal of this oxidation is critical, so this needs to be further investigated if BASE is not able to go ahead with the prefered plan of maintaining our own acid treatment for NbTi in our experiment.
Figure 19 shows a rackets made out of PVC, with NbTi wires strung along it. It is important to be made of entirely PVC such that it can be dipped in acid. This racket is made to be held from the thick rod and dipped vertically into the acid bath. The wires strung along the racket must have the insulation thoroughly removed. A racket like this is ideal since you can control the length of wire that is treated. Figure 20 shows the proposed vacuum chamber. Such a large chamber is ideal so that an entire racket with NbTi could be stored in the container without dismounting all treated wires at once.

Figure 19: A PTFE racket I made for the acid treatment of NbTi wires. **NOTE: Do not use PTFE tape in this setup. It can trap acid and lead to injury. Instead PTFE screws should be used on the bottom.**

Figure 20: Possible vacuum chamber to store the racket with NbTi wires mounted. This is needed for long term storage of wires if we are not permitted to do our own acid treatments.

4.5 New Joint Test

I was able to make one test joint using the method described in section 3.3. To make this test coil I also had to make two loading joints using the typical methods as shown in figure 17.

We were not able to make this joint operate persistently, which was expected based on the acid treatment it recieved and the issues with soldering. We had a leak in our copper tube, which causes the superconducting and non superconducting solder to mix. Another possibility is that since we only had a very short test wire, the loading joints and persistent joint were too close together, causing the system to quench immediately with a current of 200 mA.

When not in a rush, it should not be challening to prepare a properly wroking joint with this method, especially if BASE can develop acid infastructure.

5 Next Steps and Summary

This summer I was able to successfully restore the elab and the cryocooler to a state where it can be operated in a superconducting joint development program. After doing this I wrote and updated Labview code to both monitor the operation of the cryocooler for cooldown and warm-up tests, and to test any superconducting joints developed by BASE. The experimental setup and devices should remain on the cryocooler rack so that these studies can be picked up immediately by an incoming student. To continue progress towards a new BASE superconducting persistent joint I would recommend the following steps be taken.

1. Obtain the acids described in section 3.3 to treat the NbTi wire. CERN training will be required, and Stefan Ulmer should be contacted about how to best incorporate these acids into the BASE labs at CERN.
2. Conduct studies of acid treatment of NbTi wire to ensure it works as expected.
3. Now superconducting joints can be made using the new method.
4. For a proper study, parameters such as
   (a) NbTi wire thickness
   (b) Time treated under acid (different oxidation levels)
   (c) Different superconducting solders used
   (d) Time spent in solder
5. For each joint, collect data based on the program described in [4] for direct comparison with current BASE joints.

Following this program, and the joint making methods described in this report, I am confident that a superconducting joint with a critical current of 1 A can be made, allowing for the tuning of $B_1 = 0$, and a great improved towards next generation charge-to-mass and g-factor precision measurements.

Appendix

TOSHIBA HALL SENSOR GaAs ION IMPLANTED PLANAR TYPE

THS119

HIGH STABILITY MOTOR CONTROL.
DIGITAL TACHOMETER.
CRANK SHAFT POSITION SENSOR.

- Excellent Temperature Characteristics.
- Wide Operating Temperature Range. (; −55~125°C)
- Excellent Output Voltage Linearity.

Unit in mm

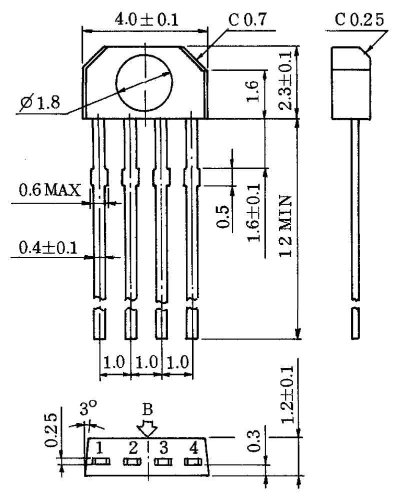

1(+) − 3(−) (INPUT)
2(+) − 4(−) (OUTPUT)

JEDEC	—
EIAJ	—
TOSHIBA	10-4B1A

Weight : 0.06g

MAXIMUM RATINGS (Ta = 25°C)

CHARACTERISTIC		SYMBOL	RATING	UNIT
Control Current	DC	I_C	10	mA
	1s		15	
Power Dissipation		P_D	150	mW
Operating Temperature Range		T_{opr}	−55~125	°C
Storage Temperature Range		T_{stg}	−55~150	°C

ELECTRICAL CHARACTERISTICS (Ta = 25°C)

CHARACTERISTIC	SYMBOL	TEST CONDITION	MIN.	TYP.	MAX.	UNIT
Internal Resistance (Input)	R_d	I_C = 5mA	450	—	900	Ω
Residual Voltage Ratio	V_{HO}/V_H	I_C = 5mA, B = 0 / B = 0.1T	—	—	±10	%
Hall Voltage (Note 1)	V_H	I_C = 5mA, B = 0.1T	55	—	140	mV
Temperature Coefficient (Note 2)	V_{HT}	I_C = 5mA, B = 0.1T T1 = 25°C, Ta = 125°C	—	—	−0.06	% / °C
Linearity (Note 3)	ΔK_H	I_C = 5mA, B1 = 0.1T, B2 = 0.5T	—	—	2	%
Specific Sensitivity (Note 4)	K*	I_C = 5mA, B = 0.1T	—	27	—	$\times 10^{-2}$ / T
Internal Resistance (Output)	R_{OUT}	I_C = 5mA	580	—	1350	Ω

Note 1 : $V_H = V_{HM} - V_{HO}$ (V_{HM} is meter indication)

Note 2 : $V_{HT} = \dfrac{1}{V_{H(T1)}} \cdot \dfrac{V_{H(T2)} - V_{H(T1)}}{T2 - T1} \times 100$ (% / °C)

Note 3 : $\Delta K_H = \dfrac{K_{H(B2)} - K_{H(B1)}}{1/2\{K_{H(B1)} + K_{H(B2)}\}} \times 100(\%)$, $K_H = \dfrac{V_H}{I_C \cdot B}$

Note 4 : $K^* = V_H / (R_d \times I_C \times B) = K_H / R_d$

V_{HO} : Residual Voltage

K_H : Product Sensitivity

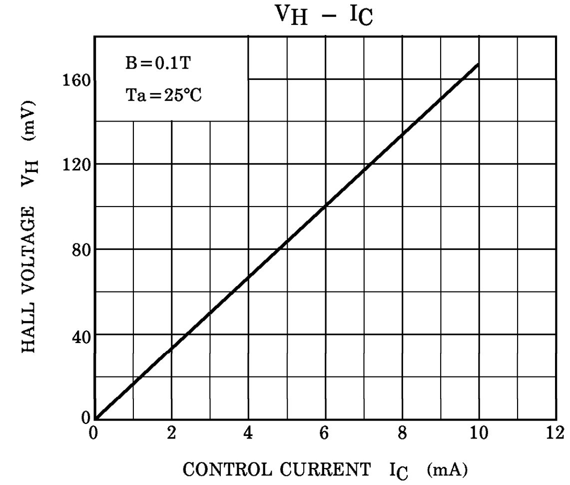
V_H – I_C
B = 0.1T
Ta = 25°C
HALL VOLTAGE V_H (mV)
0
40
80
120
160
0 2 4 6 8 10 12
CONTROL CURRENT I_C (mA)

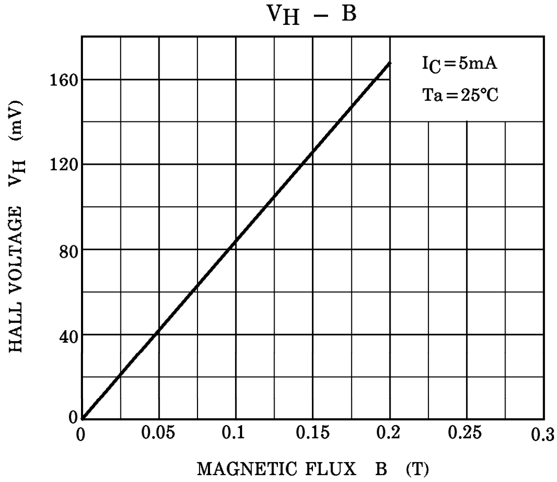
V_H – B
I_C = 5mA
Ta = 25°C
HALL VOLTAGE V_H (mV)
0
40
80
120
160
0 0.05 0.1 0.15 0.2 0.25 0.3
MAGNETIC FLUX B (T)

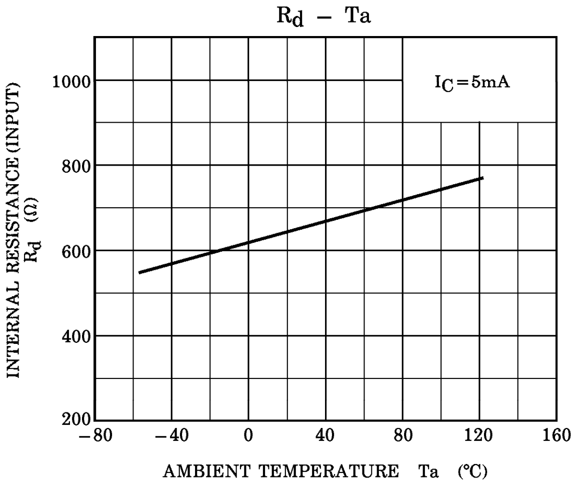
R_d – Ta
I_C = 5mA
INTERNAL RESISTANCE (INPUT) R_d (Ω)
200
400
600
800
1000
−80 −40 0 40 80 120 160
AMBIENT TEMPERATURE Ta (°C)

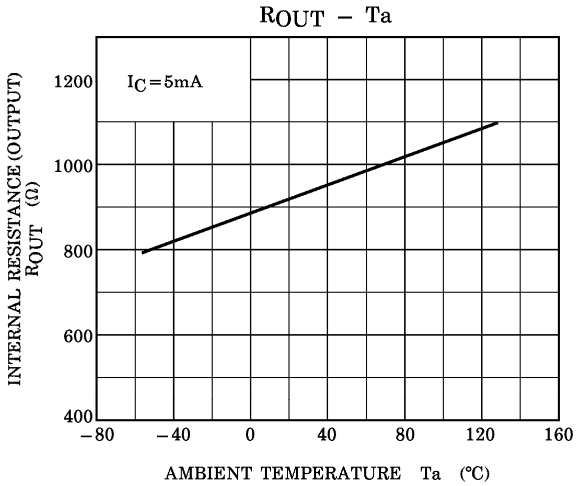
R_{OUT} – Ta
I_C = 5mA
INTERNAL RESISTANCE (OUTPUT) R_{OUT} (Ω)
400
600
800
1000
1200
−80 −40 0 40 80 120 160
AMBIENT TEMPERATURE Ta (°C)

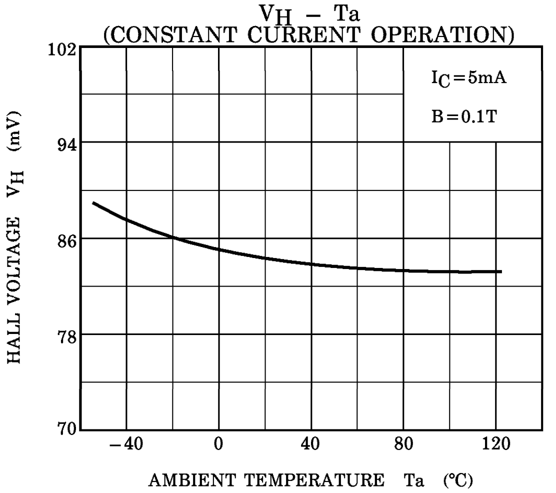
V_H – Ta
(CONSTANT CURRENT OPERATION)
I_C = 5mA
B = 0.1T
HALL VOLTAGE V_H (mV)
70
78
86
94
102
−40 0 40 80 120
AMBIENT TEMPERATURE Ta (°C)

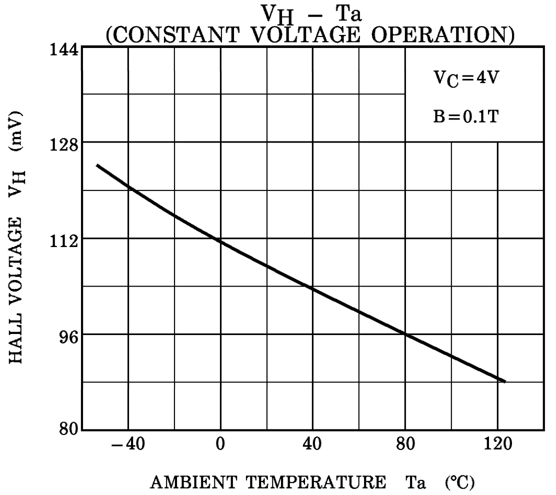
V_H – Ta
(CONSTANT VOLTAGE OPERATION)
V_C = 4V
B = 0.1T
HALL VOLTAGE V_H (mV)
80
96
112
128
144
−40 0 40 80 120
AMBIENT TEMPERATURE Ta (°C)

POLISSAGE CHIMIQUE NIOBIUM

Numéro Cuve	R-001-Nb01
Volume	400 l

PRODUITS CHIMIQUES

BCP 2.1.1 ou équivalent (mélange de H_3PO_4 50% v/v, HNO_3 25% v/v et HF 25% v/v) **r** = 1,5 kg/l (FDS EDMS 2069048)	Prêt à l’emploi

PARAMETRES DE FONCTIONNEMENT

Température d'utilisation	ambiante
pH	< 0
Vitesse d’attaque	1 µm / minute (20 °C)
Temps de traitement	Quelques minutes à plusieurs heures

Commentaires :

This is the acid treatment procedure used by the CERN superconductor acid lab. This can be work done by BASE themselves, allowing us to further study these affects.

FINAL_CODE_PC-joint-measurement-permanent-cv-read-one-probe-faster-two-temp-with-plot-joi
C:\labdata\2024\Thomas-Cryocooler\My Control Code with Joint Stuff\FINAL_CODE_PC-joint-measurement-permanent-cv-read-one-probe-faster-two-temp-with-plot-joint-heat.vi
Last modified on 16/08/2024 at 10:32
Printed on 21/08/2024 at 18:21

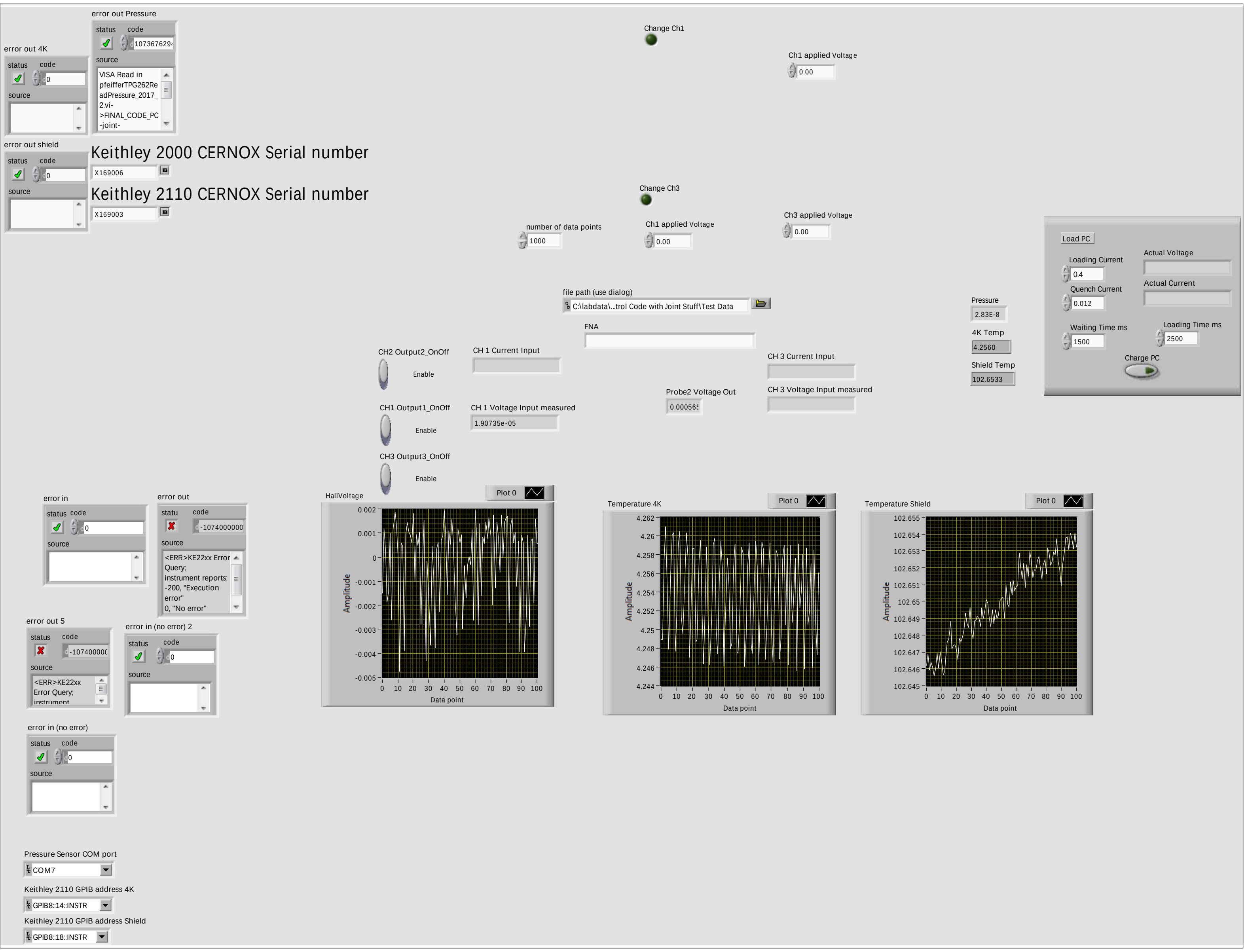

p-T-Logger_TPG262.vi

C:\COLDHEAD_CONTROL\COLDHEAD_LOG\Examples\SE\Coldhead\p-T-Logger_TPG262.vi

Last modified on 13/08/2024 at 16:55

Printed on 21/08/2024 at 19:53

Keithley 2000 GPIB address

GPIB8::14::INSTR

Keithley 2000 CERNOX Serial number

X169006

Keithley 2110 GPIB address

GPIB8::18::INSTR

Keithley 2110 CERNOX Serial number

X169003

Pressure Sensor COM port

COM7

Output file path

C:\labdata\2024\Thomas-Cryocooler\warmup

Measurement time (s)

1

Stop Measurement

Temperature

Log. scale

Pressure

Log. scale

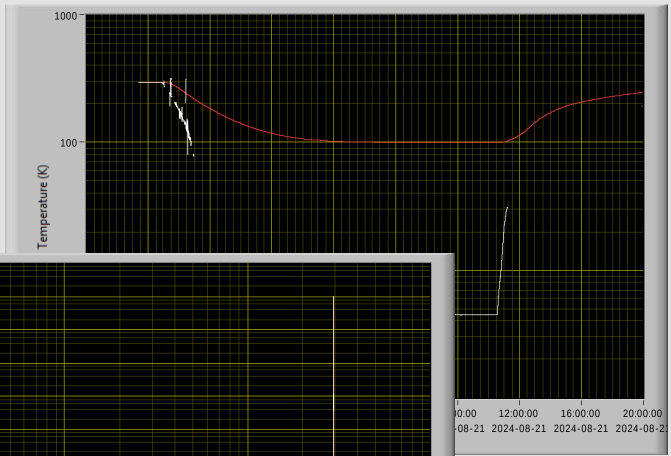

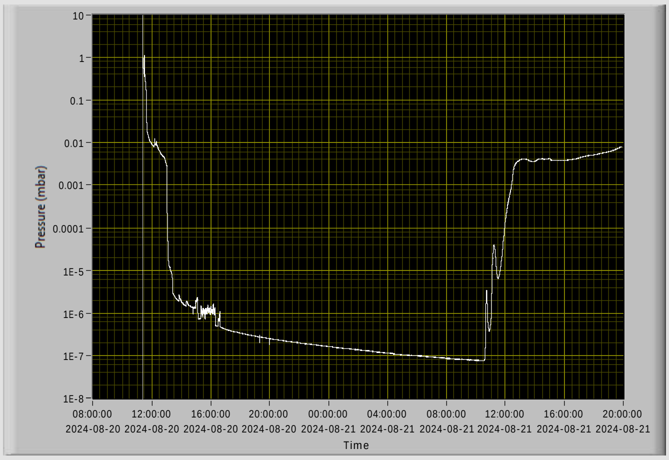

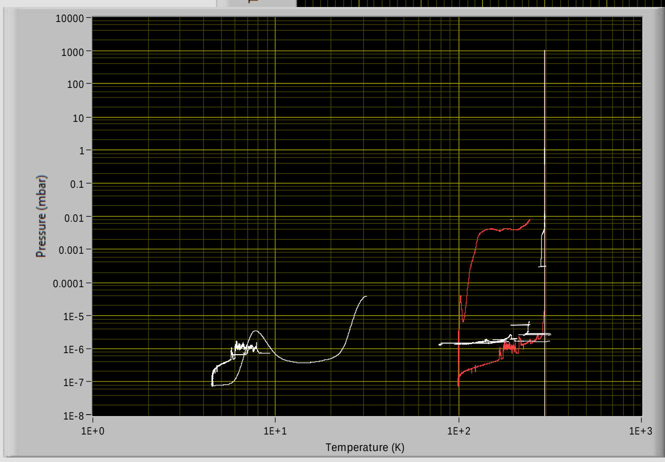

Pressure (mbar)

0.00805

Cold Head Temperature (K)

193.297

Shield Temperature (K)

245.112

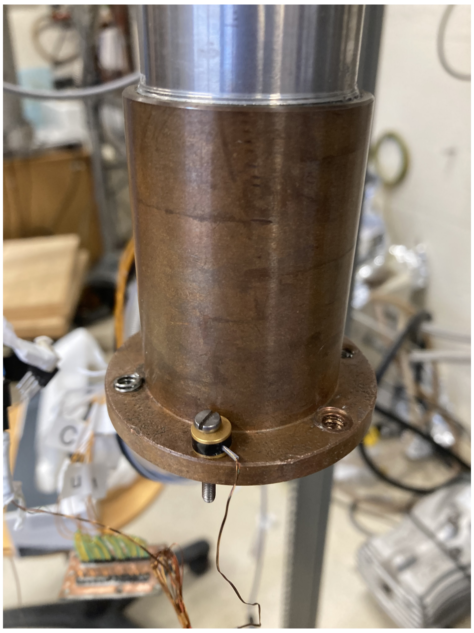

Figure 21: Picture showing the mounting position of a temperature sensor which I would refer to as "mounted on the coldhead". The test setup in not yet attached in this photo.

References

[1] Gerhart Luders. Proof of the TCP theorem. *Annals Phys.*, 2:1–15, 1957.

[2] M. J. Borchert, J. A. Devlin, S. R. Erlewein, M. Fleck, J. A. Harrington, T. Higuchi, B. M. Latacz, F. Voelksen, E. J. Wursten, F. Abbass, M. A. Bohman, A. H. Mooser, D. Popper, M. Wiesinger, C. Will, K. Blaum, Y. Matsuda, C. Ospelkaus, W. Quint, J. Walz, Y. Yamazaki, C. Smorra, and S. Ulmer. A 16-parts-per-trillion measurement of the antiproton-to-proton charge–mass ratio. *Nature*, 601(7891):53–57, January 2022.

[3] C. Smorra, S. Sellner, M. J. Borchert, J. A. Harrington, T. Higuchi, H. Nagahama, T. Tanaka, A. Mooser, G. Schneider, M. Bohman, K. Blaum, Y. Matsuda, C. Ospelkaus, W. Quint, J. Walz, Y. Yamazaki, and S. Ulmer. A parts-per-billion measurement of the antiproton magnetic moment. *Nature*, 550(7676):371–374, October 2017.

[4] Maylin Schiiffelholz. Development of a test setup to characterize persistent joints for future high precision penning trap experiments. Master's thesis, Gottfried Wilhelm Leibniz Universität Hannover, 2023.

[5] Jack A. Devlin, Elise Wursten, James A. Harrington, Takashi Higuchi, Pascal E. Blessing, Matthias J. Borchert, Stefan Erlewein, Jannek J. Hansen, Jonathan Morgner, Matthew A. Bohman, Andreas H. Mooser, Christian Smorra, Markus Wiesinger, Klaus Blaum, Yasuyuki Matsuda, Christian Ospelkaus, Wolfgang Quint, Jochen Walz, Yasunori Yamazaki, and Stefan Ulmer. Superconducting solenoid system with adjustable shielding factor for precision measurements of the properties of the antiproton. *Phys. Rev. Appl.*, 12:044012, Oct 2019.

[6] G. Gabrielse. The true cyclotron frequency for particles and ions in a penning trap. *International Journal of Mass Spectrometry*, 279(2):107–112, 2009.

[7] C. Smorra, K. Blaum, L. Bojtar, M. Borchert, K.A. Franke, T. Higuchi, N. Leefer, H. Nagahama, Y. Matsuda, A. Mooser, M. Niemann, C. Ospelkaus, W. Quint, G. Schneider, S. Sellner, T. Tanaka, S. Van Gorp, J. Walz, Y. Yamazaki, and S. Ulmer. Base – the baryon antibaryon symmetry experiment. *The European Physical Journal Special Topics*, 224(16):3055–3108, November 2015.

[8] B. M. Latacz et al. BASE—high-precision comparisons of the fundamental properties of protons and antiprotons. *Eur. Phys. J. D*, 77(6):94, 2023.

[9] Stefan Erlewein. Implementation of a superconducting shimming and shielding system in the base experiment. Master's thesis, University of Heidelberg, 2024.

[10] J. Halbritter. On the oxidation and on the superconductivity of niobium. *Applied Physics A*, 43(1):1–28, May 1987.

[11] Dipak Patel, Su-Hun Kim, Wenbin Qiu, Minoru Maeda, Akiyoshi Matsumoto, Gen Nishijima, Hiroaki Kumakura, Seyong Choi, and Jung Ho Kim. Niobium-titanium (Nb-Ti) superconducting joints for persistent-mode operation. *Scientific Reports*, 9(1):14287, October 2019.

[12] Lukas Wolf. Developments for the setup and operation of the base-cdm experiment. Master's thesis, Heinrich Heine Universitat Dusseldorf, 2024.